

Flow Dynamics around Tandem Cylinders with Different Longitudinal Gaps

^[1] Deep Pandya, ^[2] Atal Harichandan^{[1][2]} Mechanical Engineering, Marwadi Education Foundation Group of Institutions, Rajkot, India

Abstract: -- Dynamics of flow around three circular cylinders in the tandem arrangement has been investigated. Finite volume method has been employed to perform the simulations with high accuracy at Reynolds numbers $Re = 100$ and $Re = 200$. A consistent flux reconstruction scheme is considered for the explicit calculation of the primitive variables in flow domain. Due to the complexity of flow geometry, unstructured grids with triangular cells are employed for numerical simulations. The influence of longitudinal gaps ($L = 2D$ and $L = 3D$) between cylinders upon flow characteristics are estimated. Streamlines and vorticity contours along with a periodic variation of lift and drag coefficients are discussed for each cylinder in the tandem configuration. The downstream cylinder in the configuration experiences very large unsteady forces that can give rise to wake-induced flutter. Also, with an increase in the longitudinal gap, flow separation or reattachment of the shear layer from the upstream cylinder to the immediate downstream cylinder are not observed. In the tandem arrangement of cylinders, the flow field behind the downstream cylinder develops from the steady state into an unsteady state as Reynolds number increases.

Keywords: Flow dynamics; finite volume method, tandem arrangement; longitudinal gap, vorticity contours, streamlines.

I. INTRODUCTION

Many engineering structures such as offshore risers, pipelines, cooling systems for power plants, buildings, chimneys, tubes in heat exchangers, and transmission lines involve multiple bluff bodies in proximity. Depending on the configuration of these bodies, a wide variety of interference phenomena can be observed. Even the simplest case of two identical cylinders presents a rich spectrum of different flow features. The difficulty in predicting flow around multi-cylinders is increased when two or more of these cylinders are placed in proximity to each other. This is because the dynamic interaction between the shed vortices, shear layers and Karman vortex streets appears in the wake of the cylinders. The exact form of the interaction is strongly dependent on the Reynolds number of the flow and on the arrangement of the cylinders. The geometrical configurations of two or more circular cylinders can be categorized in general into side-by-side, tandem and staggered arrangements with respect to the direction of the free stream flow. These configurations have been studied experimentally and numerically by several researchers in the past. Zdravkovich [1] suggested that the flow phenomena differ a lot when different longitudinal gaps are considered between tandem cylinders for the case of unconfined flow. When the longitudinal gap (L) between the cylinders is within the critical gap range ($1.1D < L < 2.2D$), the

unsteady behavior initially produced. However for critical gap with increase in Reynolds number, the flow field between the cylinders becomes marginally unsteady. Flow behind the downstream cylinder becomes unsteady and a sparse Karman vortex street is formed. In the present research work, numerical results of flow past three cylinders tandem arrangements with different longitudinal gaps are discussed in details. The two-cylinder flow bears similarity to flow over more-than-two circular cylinders in many aspects such as synchronization and merging of wakes, deflection and flip-flopping of the gap flows, and narrow-wide wake structures. However, the two cylinder flow may not be entirely representative of flows over more number of cylinders because they exhibit quite disparate behaviors as explained by Sumner et al. [2] and Zhang and Zhou [3]. Therefore, numerical simulations are also performed over three circular cylinders in tandem arrangements with various longitudinal gaps at $Re = 100$ and 200 . In order to get better understanding of the wake interference around multiple cylinders, the results obtained for flow past a single cylinder is taken as a reference for analysis.

II. GOVERNING EQUATIONS

The physical problem considered in the present study is a two-dimensional boundary layer flow of an incompressible fluid around a three circular cylinders in tandem placed in a uniform flow domain.

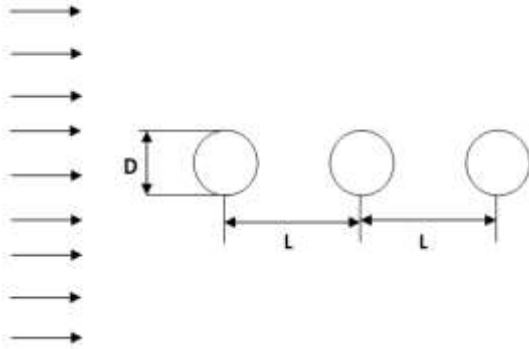


Figure 1. Geometrical depiction of flow domain

A two-dimensional boundary-layer flow is generated from an incident uniform fluid stream flowing over three circular cylinders in tandem at zero incidences. U_∞ is the uniform velocity of the fluid outside the boundary layer thickness. The equations governing incompressible viscous fluid flow in two-dimensions are the Continuity equation and the two components of Momentum equation. In absence of body forces and heat transfer, these equations can be expressed in the conservative non-dimensional primitive variable form as follows:

Continuity equation:

$$\frac{\partial u}{\partial x} + \frac{\partial v}{\partial y} = 0 \quad (1)$$

X - Momentum equation:

$$\frac{\partial u}{\partial t} + \frac{\partial(u^2)}{\partial x} + \frac{\partial(uv)}{\partial y} = -\frac{\partial p}{\partial x} + \frac{1}{\text{Re}} \times \left(\frac{\partial^2 u}{\partial x^2} + \frac{\partial^2 u}{\partial y^2} \right) \quad (2)$$

Y - Momentum equation:

$$\frac{\partial v}{\partial t} + \frac{\partial(uv)}{\partial x} + \frac{\partial(v^2)}{\partial y} = -\frac{\partial p}{\partial y} + \frac{1}{\text{Re}} \times \left(\frac{\partial^2 v}{\partial x^2} + \frac{\partial^2 v}{\partial y^2} \right) \quad (3)$$

Where the velocity components u and v are in the x - and y -directions, respectively, p is ratio of pressure and density, Re is the Reynolds number and t is the non-dimensional time. The governing equations have been non-dimensionalized by considering the diameter of the cylinder as the length scale (D) and the free-stream velocity, U_∞ , for the velocity scale.

In the present calculations, free stream values for pressure and velocity are assigned as the initial values to each triangular cell in the domain. Continulative boundary conditions are used at the outlet boundary. For unconfined

flow simulations, the inlet, outlet, top and bottom boundaries of the rectangular domain are kept far away from the body surface. On the body surface, no slip condition is applied. In the present flow-solver, CFRUNS (Harichandan and Roy [4]) has been implemented to solve the full Navier-Stokes equations numerically in the physical plane itself without using any transformation to the computational plane. The flux reconstruction cell on the face of the control volume is placed centrally between the two cells which share that face. The cell face center velocities are reconstructed explicitly by solving the momentum equations on flux reconstruction control volumes defined judiciously around the respective cell face centers. This is followed by solution of the cell centre pressure field using a discrete Poisson equation developed from the reconstructed velocities and updating the cell centre velocities by using an explicit scheme.

III. NUMERICAL RESULTS

In this paper, the CFRUNS method is first applied to simulate flow past a circular cylinder placed in a uniform flow at zero angle of incidence. Subsequently, flow calculations are performed for three circular cylinders in tandem with different longitudinal gaps ($L = 2D$ and $5D$) between them. Streamlines and vorticity contours are plotted as the flow visualization aids. Some parameters characterizing the flow aspects such as lift and drag coefficients and Strouhal number are also computed and quantitatively compared with the results of other researchers. In the present case, flow is assumed to be two-dimensional and laminar in all possible arrangement of cylinders. Non-dimensional time step used for all the simulations is 0.0005. At every time level, the convergence criteria for pressure-Poisson equation is set in a manner that the residual is less than 10^{-6} . The CFRUNS scheme is second-order accurate. The spatial accuracy of the scheme is verified by solving Couette flow for which exact solution is available. Convergence characteristics of CFRUNS scheme is tested for unconfined flow past a circular cylinder.

A. Unconfined flow past a circular cylinder

For flow past a cylindrical body when Reynolds number increases beyond a certain critical value (≈ 48), instabilities develop in the flow which trigger asymmetry in the vortex structure formed in the rear portion of the cylinder surface. Subsequently alternate separation of vortices from upper and lower portions of the cylinder gets initiated. All these destabilizing effects are absent in the flow field until and unless they are introduced artificially. As the geometry of the flow as well as the initial and boundary conditions are symmetric, the Navier-Stokes equations should produce

symmetric solution even for Reynolds number greater than 48. However, the truncation and round-off errors as well as errors produced due to the numerical approximation scheme act as perturbing factors and eventually trigger the vortex shedding phenomenon. In the following paragraphs some numerical results of the present study conducted on flow past a circular cylinder using the CFRUNS scheme is discussed. In the present study, the unsteady flow at $Re = 100$ and 200 is simulated on a triangular mesh comprising of 29,464 cells and 14,878 nodes for circular cylinder. The unstructured triangular grid has been generated using GAMBIT software and used as input to the CFRUNS solver. There are 160 nodes on the body as chosen suitably from the grid independence test. In either case, the cylinder is placed in a rectangular domain in which the upper and lower boundary, inlet boundary and outlet boundary are kept at distances of $15D$, $10D$ and $30D$ respectively from the centre of the cylinder.

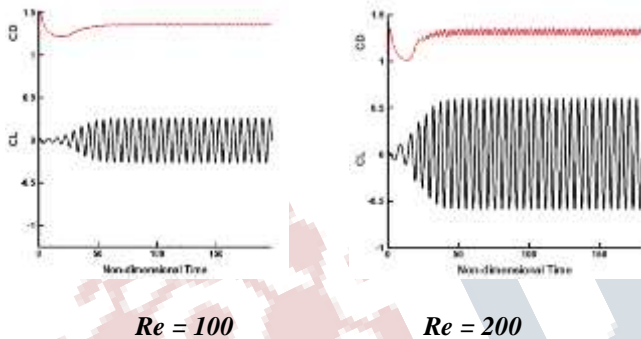


Figure 2. Lift and drag coefficients for flow past single circular cylinder at $Re = 100$ and 200

periodicity illustrated in lift and drag coefficients implies the periodic vortex shedding from the rear surface of the cylinder. Table 1 lists mean value and amplitude of drag and lift coefficients and Strouhal number of present results as well as other published numerical results at $Re = 100$.

Table 1. Values of flow parameters for single circular cylinder at $Re = 100$ and 200

Parameters	Lift coefficient (CL)		Drag coefficient (CD)		Strouhal number (St)	
	$Re=100$	$Re=200$	$Re=100$	$Re=200$	$Re=100$	$Re=200$
Ding et al. [7]	± 0.287	± 0.659	1.356 ± 0.010	1.348 ± 0.05	0.166	0.196
Hanichandan & Roy (2010)	± 0.278	± 0.602	1.352 ± 0.010	1.320 ± 0.05	0.161	0.192
Present result	± 0.259	± 0.607	1.344 ± 0.010	1.311 ± 0.05	0.162	0.193



Figure 3. Vorticity and streamlines contours for $Re = 100C$

Figure 4. Vorticity and streamlines contours for $Re = 200$

Cylinders, development and shedding of asymmetric vortices from the multiple cylinder surfaces due to the multiple body wakes are some of the interesting flow features needing necessary exploration. Keeping this phenomenon in mind, in the present work, two cylinders in tandem are considered with $L=2D$ (within critical gap range) and $L = 5D$ (beyond critical gap range). In both the cases, we have conducted numerical simulations at $Re = 100$ and 200 and gap spacing of 1.0 . All the flows considered in the present study are assumed to be

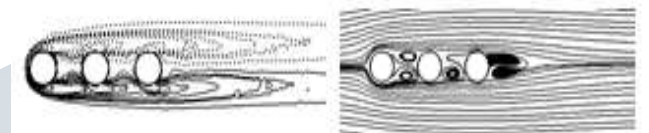


Figure 5. Vorticity contours and streamlines of flow past three circular cylinders in tandem ($L = 2D$) at $Re = 100$



Figure 6. Vorticity contours and streamlines of flow past three circular cylinders in tandem ($L = 2D$) at $Re = 200$

Figures 5 and 6 present the vorticity contours and streamlines of flow past three cylinders in tandem for $L = 2D$ at $Re = 100$ and 200 , respectively at instantaneous non-dimensional time $t = 250$. It is observed that at $Re = 100$, the flow maintains a steady state though the Reynolds number is much greater than the critical value for single cylinder ($Re = 48$). From the streamline plots for $Re = 100$, it is observed that the flow in the gap region between the cylinders is rather restricted. Also, the shear layer which is separated from the inside surface of the upstream cylinder reattaches onto the outer surface of the middle cylinder. The same phenomenon also occurs between middle cylinder and downstream cylinder. This flow regime has been classified by Zdravkovich (1977) as the steady reattachment. Figure 7 shows the temporal histories of drag and lift coefficients for flow past three tandem cylinders at $Re = 100$ and 200 , respectively. It can be observed that amplitude of lift coefficient remains almost equal to zero even after sufficient numbers of time-steps. It implies that the unsteady behavior initially produced by the artificial numerical perturbation due to round off errors etc., is gradually dissipated by viscosity. However, with increase in Reynolds number (Re

= 200), the flow field between the cylinders (upstream-middle and middle-downstream) becomes marginally unsteady. Flow behind the downstream cylinder becomes unsteady and a sparse Karman vortex street is formed. This gap ($L = 2D$) falls in the critical gap regime as proposed by Williamson [5] and, therefore, the streamline and vorticity contours and the temporal behavior of lift and drag coefficients for $Re = 200$ case are as per expectation. The results for the three cylinders in tandem arrangement are indicated by associating a number along with CL and CD. '1' stands for the upstream cylinder, '2' stands for the middle cylinder and '3' stands for the downstream cylinder.

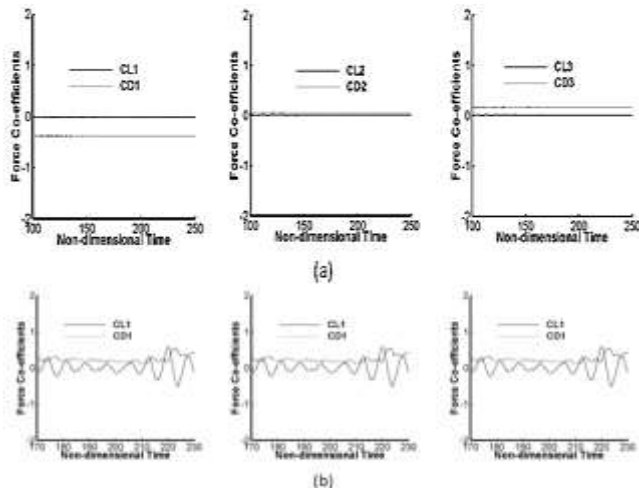


Figure 7. Lift and drag coefficients of flow past three circular cylinders in tandem ($L = 2D$) at $Re = 100$ and 200
For cylinders in tandem arrangement, the upstream cylinder experiences higher drag than the other two cylinders. The drag coefficient for the downstream cylinder is very low as compared to the other upstream cylinders due to the sparse Karman vortex street behind it. With lower transverse gap ($T = 2D$) from our results. With flip-flopping wake pattern at such a low transverse gap, FFT of the lift coefficient does not produce any distinct dominant frequency. For cylinders in tandem arrangement, the steady wake pattern obtained at $Re = 100$ has no vortex shedding frequency. At $Re = 200$, due to flip-flopping nature of wake patterns, any distinct dominant frequency is not obtained from the FFT analysis of the lift coefficient. Therefore, no shedding frequency is mentioned for three cylinders in tandem arrangement at such a low longitudinal gap between the cylinders

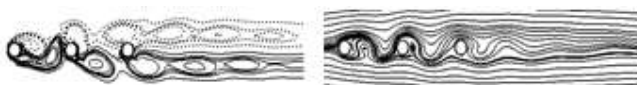


Figure 8. Vorticity contours and streamlines of flow past three circular cylinders in tandem ($L = 5D$) at (a) $Re = 100$



Figure 9. Vorticity contours and streamlines of flow past three circular cylinders in tandem ($L = 5D$) at $Re = 200$

It has been a difficult task to conclude on the nature of the flow behind the cylinders with such low separation gaps which lie within critical gap region. In order to obtain a distinct flow pattern behind the cylinders, numerical simulations were subsequently performed for the case of $L = 5D$ for tandem arrangement of three circular cylinders. The non-dimensional time step used is 0.0005. In the present study, the unsteady flow at $Re = 100$ and 200 are simulated on a triangular mesh with 25,180 cells and 12,840 nodes for $L = 5D$ case

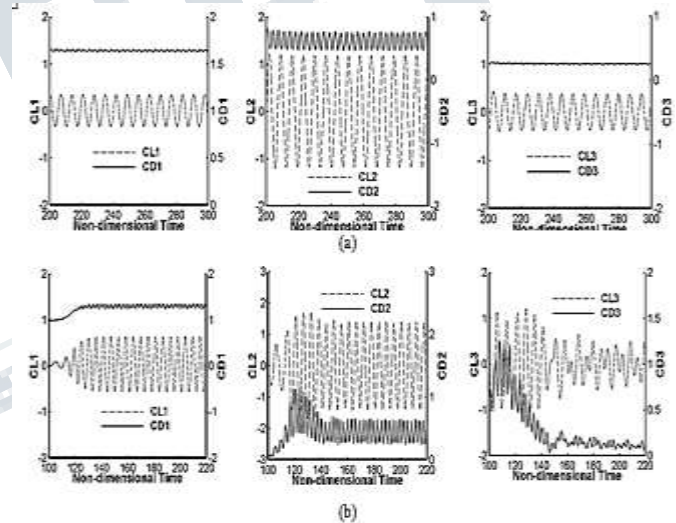


Figure 10. Lift and drag coefficients of flow past three circular cylinders in tandem ($L = 5D$) at (a) $Re = 100$ and (b) $Re = 200$

Figures 8 and 9 present the vorticity contours and streamlines of flow past three circular cylinders in tandem for $L = 5D$ at $Re = 100$ and 200 , respectively at instantaneous non-dimensional time $t = 220$. When the longitudinal gap between the cylinders is increased to $5D$, the flow pattern in the gap region experiences a distinct change. The phenomenon involving the separation and reattachment of shear layer from the upstream cylinder to the immediate downstream cylinder is no more prevalent for the present case. Instead, Karman vortex streets are observed between the cylinders. From the vorticity contours, it is observed that the vortex shedding from the downstream

cylinder is highly disturbed by the impingement of the vortex streets emerging from upstream and middle cylinders. The temporal histories of lift and drag coefficients are shown in Figures 10 (a) and (b). It can be seen that the synchronization occurs between the impingement flow and vortex shedding from the downstream cylinder. It is observed that the Strouhal number value remains same for all the cylinders at a particular Reynolds number in either of the arrangements. This phenomenon agrees well with the results of Liang et al. [6]

IV. CONCLUSION

In the present study an incompressible two dimensional Navier-Stoke solver is developed based on the fully explicit finite volume scheme. The flow is considered unsteady, viscous, laminar and two dimensional. The solver is first validated for flow past the single circular cylinder at Reynolds number of $Re = 100$ and 200 . The results are in good agreement with other researchers which indicates the good convergence and accuracy of the present solver. For the case of flows past three cylinders in tandem, it is observed that the downstream cylinder experiences very large unsteady forces This phenomenon is more likely to occur with less longitudinal gap between the cylinders. With relatively lower longitudinal gap ($L = 2D$), steady wake pattern was obtained at $Re = 100$ but sparse Karman street was observed at $Re = 200$. In this case, any distinct dominant shedding frequencies were not obtained by the FFT analyses of the lift coefficients. When the longitudinal gap was increased ($L = 5D$), there were no flow separation or reattachment of shear layer from the upstream cylinder to the immediate downstream cylinder. Instead, Karman vortex streets were observed between the cylinders. However, the vortex shedding from the downstream cylinder was highly disturbed by the impingement of the upstream vortex streets emerging from upstream and middle cylinders. The vortex shedding frequency strongly depended on the gap spacing. The FFT analyses of the lift coefficients show distinct identical vortex shedding frequencies for all the cylinders.

REFERENCES

- [1]. Zdravkovich, M.M., 1985. Flow induced oscillations of two interfering circular cylinders. *J. Sound Vib.* 101, 511–521.
- [2]. Sumner D., Wong S.S.T., Price S.J. and Paidoussis M.P. (1999): Fluid behavior of side-by-side circular cylinders in steady cross-flow. *J. of Fluids and Structures*, Vol. 13, pp. 309-338.
- [3]. Zhang H.J. and Zhou Y. (2001): Effect of unequal cylinder spacing on vortex streets behind three side-by-side cylinders. *Phy. of Fluids*, Vol. 13, No. 12, pp. 3675-3686.
- [4]. A. B. Harichandan. and A. Roy (2010): Numerical investigation of low Reynolds number flow past two and three circular cylinders using unstructured grid CFR scheme, *International Journal of Heat and Fluid Flow*, Vol. 31, pp. 154–171.
- [5]. Williamson, C.H.K., 1985. Evolution of a single wake behind a pair of bluff bodies. *J. Fluid Mech.* 159, 1–18.
- [6]. Liang C., Papadakis G. and Luo X. (2009): Effect of tube spacing on the vortex shedding characteristics of laminar flow past an inline tube array: A numerical study. *Computers and Fluids*, Vol. 38, pp. 950-964.
- [7]. Ding, H., Shu, C., Yeo, K.S., Xu, D., 2007. Numerical simulation of flows around two circular cylinders by mesh-free least square-based finite difference methods. *International Journal for Numerical Methods in Fluids* 53, 305–332